Rapid Communications

Crystal and magnetic structures of magnetic topological insulators $MnBi_2Te_4$ and $MnBi_4Te_7$

Lei Ding,[1,*] Chaowei Hu,[2] Feng Ye,[1] Erxi Feng,[1] Ni Ni,[2] and Huibo Cao[1,†]

[1]*Neutron Scattering Division, Oak Ridge National Laboratory, Oak Ridge, Tennessee 37831, USA*

[2]*Department of Physics and Astronomy and California NanoSystems Institute, University of California, Los Angeles, California 90095, USA*

(Received 6 September 2019; published 27 January 2020; corrected 26 May 2020)

Using single-crystal neutron diffraction, we present a systematic investigation of the crystal structure and magnetism of the van der Waals topological insulators $MnBi_2Te_4$ and $MnBi_4Te_7$, where rich topological quantum states have been recently predicted and observed. Structural refinements reveal that considerable Bi atoms occupied on the Mn sites in both materials, distinct from the previously reported antisite disorder. We show unambiguously that $MnBi_2Te_4$ orders antiferromagnetically below 24 K, featured by a magnetic symmetry R_I-3c, while $MnBi_4Te_7$ is antiferromagnetic below 13 K with a magnetic space group P_c-3c1. They both present antiferromagnetically coupled ferromagnetic layers with spins along the c axis. We put forward a stacking rule for the crystal structure of an infinitely adaptive series $MnBi_{2n}Te_{3n+1}$ ($n \geqslant 1$) with a building unit of [Bi_2Te_3]. By comparing the magnetic properties between $MnBi_2Te_4$ and $MnBi_4Te_7$, together with recent density-functional theory calculations, we concluded that a two-dimensional magnetism limit might be realized in the derivatives. Our work may promote theoretical studies of topological magnetic states in the series of $MnBi_{2n}Te_{3n+1}$.

DOI: 10.1103/PhysRevB.101.020412

Introduction. In condensed matter physics, van der Waals (vdW) magnetic heterostructures stacked layer by layer in a controlled sequence have attracted a great deal of interest as they have been found to show exotic physical properties and emergent phenomena [1–4]. Novel properties in these materials can be controlled by tuning the stacked atomic layers, paving the way for designing new quantum materials [1]. The vdW magnetic topological insulators have been suggested as a promising material platform for the exploration of exotic topological quantum phenomena such as the quantum anomalous Hall effect (QAHE), Majorana fermions, as well as topological magnetoelectric effects [4–7]. However, a homogeneous heterostructure with intrinsic magnetism, an ideal platform for studying such topological quantum effects, is experimentally elusive [4].

Very recently, $MnBi_2Te_4$ was proposed to be the first intrinsic antiferromagnetic (AFM) topological insulator [7–17]. It has been shown that below 24 K, $MnBi_2Te_4$ orders into an A-type magnetic structure based on magnetic properties, density-functional theory calculations, and powder neutron diffraction measurements [7,13,14,18]. Since such a spin configuration breaks the product (S) of the time-reversal symmetry and the primitive-lattice translational symmetry at the (001) surface, it is expected that a gapped surface Dirac cone can be observed by angle-resolved photoemission spectroscopy (ARPES) made on a cleaved (001) surface [5,12]. However, both gapped and gapless [8,11,13,15] Dirac cones have been observed in ARPES measurements. This casts doubt on the magnetic configuration determined using the powder neutron diffraction data [7]. Furthermore, a new family of $MnBi_{2n}Te_{3n+1}$ ($n = 2, 3$) was later discovered [19,20]. Among them, $MnBi_4Te_7$ [19,21,22] and $MnBi_6Te_{10}$ [19] have been suggested to be new magnetic topological insulators with weak interlayer magnetic coupling through combined ARPES and first-principles calculations [21]. Although the A-type AFM was suggested for $MnBi_4Te_7$ by its anisotropic magnetic properties, a neutron experiment to prove it has yet to be reported. Another riddle in both $MnBi_2Te_4$ and $MnBi_4Te_7$ is the saturated magnetic moment that is found to be about $3\mu_B$ in both cases [15,17,21,22]. This is significantly smaller than $5\mu_B$ expected for the Mn^{2+} ion. To elucidate this reduction and unambiguously determine their magnetic structures, a single-crystal neutron diffraction experiment, which can map out the complete magnetic reflections with a better resolution, is urged.

Defects are of great importance in optimizing and understanding the surface states and magnetism in magnetic topological insulators [23,24]. Antisite defects in $MnBi_{2n}Te_{3n+1}$ have been found to be divergent. For example, by combining single-crystal x-ray diffraction and electron microscopy, Zeugner *et al.* have shown the presence of antisite disorder between Mn and Bi sites and Mn vacancies in the nominal $MnBi_2Te_4$ which yields the composition $Mn_{0.85(3)}Bi_{2.10(3)}Te_4$ [14], while Yan *et al.* later found the cationic disorder with only about 3% of the Bi sites occupied by Mn estimated by scanning tunneling microscopy [18]. Similar defects have been reported in the nominal $MnBi_4Te_7$ by x-ray diffraction and transmission electron microscopy [20,22]. However, in light of the great difference between Mn and Bi in electronegativity, antisite defects are basically unfavorable. To rationally sort out the debate, it is natural to employ a neutron diffraction technique as Mn and Bi atoms have an opposite sign of the neutron scattering length.

Beyond the investigation of the magnetic structures, motivated by the above-mentioned discoveries, our work is devoted to setting up the relationship between the crystal

*dingl@ornl.gov
†caoh@ornl.gov

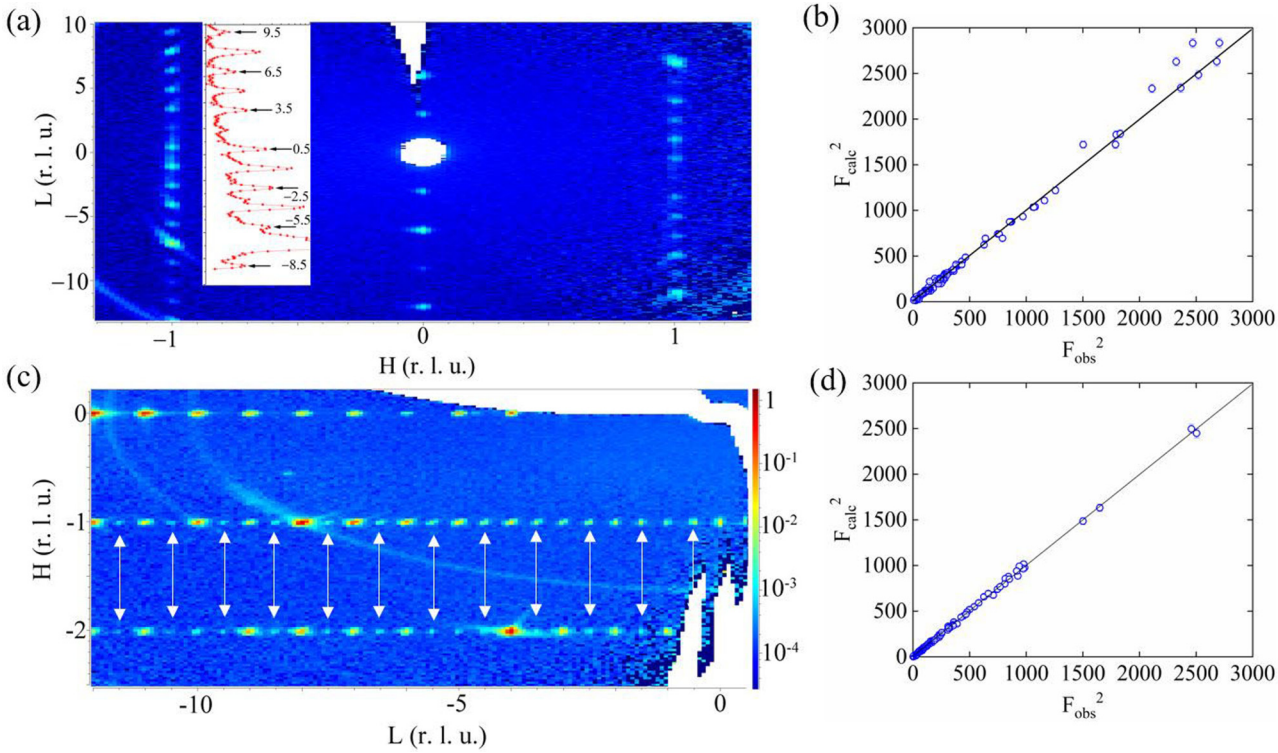

FIG. 1. (a) Contour map of neutron intensity of $MnBi_2Te_4$ in the ($H0L$) reciprocal plane at 7 K measured on CORELLI. (b) The results for the nuclear and magnetic structure refinements of $MnBi_2Te_4$ at 4.5 K with neutron data from DEMAND. (c) Contour map of neutron intensity of $MnBi_4Te_7$ in the ($H0L$) reciprocal plane at 7 K measured on CORELLI. Arrows mark the magnetic reflections. (d) The results for the nuclear and magnetic structure refinements of $MnBi_4Te_7$ at 4.5 K with neutron data from DEMAND.

structure and magnetic properties by examining the simple lattice-stacking rule starting from the prototype topological insulator Bi_2Te_3 [25,26]. Conventionally, its structure is described by the stacking of three "quintuple-layer" building blocks [23,27]. The bond coupling is rather strong between the two atomic layers within one quintuple layer, but much weaker, predominantly of the vdW type, between the neighboring quintuple layers. Yet, the "quintuple-layer" stacking description does not reflect the structural symmetry of Bi_2Te_3 that may be important in understanding the topological properties in $MnBi_{2n}Te_{3n+1}$. The proposed stacking rule for building a magnetic topological insulator Mn-Bi-Te series in this work practically captures the structural symmetry, reflects the precise layer stacking sequence, and reveals an infinitely adaptive series, stimulating theoretical calculations of the exotic quantum states in the series of $MnBi_{2n}Te_{3n+1}$.

Crystal structures of $MnBi_2Te_4$ and $MnBi_4Te_7$. We examined the crystal structure of both powder and single-crystalline $MnBi_2Te_4$ and $MnBi_4Te_7$ samples using x-ray and neutron diffraction techniques [28]. For $MnBi_2Te_4$, the slice view of the neutron diffraction data at 7 K is shown in Fig. 1(a) while the powder x-ray diffraction pattern is presented in the Supplemental Material [29]. For $MnBi_4Te_7$, Fig. 1(c) shows the contour map of neutron diffraction at 7 K, where the presence of sharp reflections indicates the high quality of the crystal. Single-crystal neutron diffraction was also performed on the HB-3A DEMAND diffractometer [30,31] at room temperature on the same crystals [29]. We have refined both the single-crystal neutron diffraction data from DEMAND and x-ray powder diffraction data using the FULLPROF software [32], which shows that $MnBi_2Te_4$ and $MnBi_4Te_7$ crystallize in R-3m and P-3m1 space group, respectively. The refinement results as well as structural parameters are shown in Fig. 1 and Tables S1–S4 [29], respectively. The refined lattice parameters are presented in Table I, which are in good agreement with previous reports [19,33]. Our refinement shows that about 18(1)% of Bi is occupied at the Mn sites in the as-grown crystal $MnBi_2Te_4$ whereas there is negligible Mn 1(1)% residing on the Bi sites [29]. This sort of nonstoichiometry effect becomes more robust in the $MnBi_4Te_7$ crystal where there is 27.9(4)% of Bi on the Mn sites. Such results are substantially different from the intermixing between Mn and Bi sites and vacancies of Mn in $MnBi_2Te_4$ and $MnBi_4Te_7$ documented previously [13,14,18,20,22].

Thermodynamic properties of $MnBi_2Te_4$ and $MnBi_4Te_7$. The zero-field-cooling (ZFC) temperature-dependent magnetic susceptibilities of $MnBi_2Te_4$ and $MnBi_4Te_7$ measured with the field parallel to the c axis are shown in Fig. 2. For the $MnBi_2Te_4$ case, the susceptibility first increases with decreasing temperature and exhibits a sharp cusp at $T_N = 24$ K, signaling the AFM ordering. In order to further characterize the magnetic phase transition, we measured the specific heat of $MnBi_2Te_4$. As shown in Fig. 2(b), the cusp at 24 K is indicative of the AFM transition, in good agreement with the magnetic susceptibility data. Thus $MnBi_2Te_4$ only undergoes one AFM transition at 24 K. The magnetic susceptibility of $MnBi_4Te_7$ shows a sharp peak at $T_N = 13$ K [Fig. 2(c)], indicating an AFM transition. The nature of the transition can

TABLE I. Derivatives of the vdW $MnBi_{2n}Te_{3n+1}$ topological insulators. Lattice parameters (i: experiment; ii: prediction) are shown at room temperature. The lattice parameters for each sequence of the stacking units are based on Bi_2Te_3: $a = b = 4.3896(2)$ Å, $c = 30.5019(10)$ Å [27]. When $n = 2 + 3m$ ($m = 0, 1, 2\ldots$), the lattice of derivatives is primitive. The predicted magnetic space groups (MSGs) are made based on a symmetry analysis using the **k** vectors of (0, 0, 3/2) for the rhombohedral lattice, (0, 0, 1/2) for the hexagonal lattice, and (0, 0, 0) for the cases with ferromagnetic (FM) order.

n	Sequence	SG	Lattice parameter		Magnetic properties and MSG
1	*M*-C-*M*-B-*M*-A-*M*	*R*-3*m*	4.3336(2) Å	40.926(3) Å [i, this work]	AFM, R_I-3*c* [i, this work]
2	A-*M*-C	*P*-3*m*1	4.3453(5) Å	23.705(3) Å [i, this work] 23.81 Å [ii]	AFM, *Pc*-3*c*1 [i, this work]
3	*M*-C-A-B-*M*-A-B-C-*M*-B-C-A-*M*	*R*-3*m*	4.3745(3) Å	101.985(8) Å [i] [19] 101.94 Å [ii]	AFM, R_I-3*c* / FM, *R*-3*m*′ [ii]
4	*M*-C-A-B-C-*M*-B-C-A-B-*M*-A-B-C-A-*M*	*R*-3*m*		132.45 Å [ii]	AFM, R_I-3*c* / FM, *R*-3*m*′[ii]
5	*M*-C-A-B-C-A-*M*	*P*-3*m*1		54.32 Å [ii]	AFM, P_c-3*c*1 / FM *P*-3*m*′1[ii]
6	*M*-C-A-B-C-A-B-*M*-A-B-C-A-B-C-*M*-B-C-A-B-C-A-*M*	*R*-3*m*		193.47 Å [ii]	AFM, R_I-3*c* / FM, *R*-3*m*′ [ii]

be cross-checked by the specific heat data of $MnBi_4Te_7$. As shown in Fig. 2(d), the specific heat shows a small anomaly at 13 K, consistent with the magnetic susceptibility results and the previous results [21,22]. The Neél temperature of $MnBi_4Te_7$ is about two times smaller than that of $MnBi_2Te_4$.

A-type magnetic structure of $MnBi_2Te_4$ and $MnBi_4Te_7$. The magnetic structure of $MnBi_2Te_4$ has been previously investigated using powder neutron diffraction [18]. They found that the AFM structure has the magnetic symmetry P_c-3*c*1 (BNS symbol) [34] propagated by a vector $\mathbf{k} = (0, 0, 1/2)$, which is a lower magnetic symmetry than that determined from our neutron data. As shown in Fig. 1(a), our neutron diffraction experiment reveals that a set of magnetic reflections, which appears at 7 K, can be indexed by a vector $\mathbf{k} = (0, 0, 3/2)$. As a matter of fact, the magnetic reflections shown in Ref. [18] should be reasonably indexed by this vector, implying that the proposed magnetic space group should be reconsidered here. To solve the magnetic structure of $MnBi_2Te_4$, we have carried out the magnetic symmetry analysis by considering the **k** vector and the parent space group *R*-3*m*1′ with help of the ISODISTORT software [35] and the Bilbao Crystallography Server [36]. There are two active magnetic irreducible representations, mT2+ and mT3+. After testing these candidates, we found the irrep mT2+, corresponding to the magnetic space group R_I-3*c*, is the only solution, while the latter irrep mT3+ conveying three different magnetic structures is incompatible with our neutron data [29]. Magnetic neutron diffraction data measured at 4.5 K on DEMAND were then refined using the magnetic symmetry R_I-3*c* and the results of the refinement are shown in Fig. 1(b). It turns out that spins line up ferromagnetically in the *ab* plane below 24 K whereas between layers, magnetic moments are antiparallel. The refined magnetic moment of Mn^{2+} at 4.5 K is $4.7(1)\mu_B$, in good accordance with the expected totally ordered moment $5\mu_B$ for the Mn^{2+} ion.

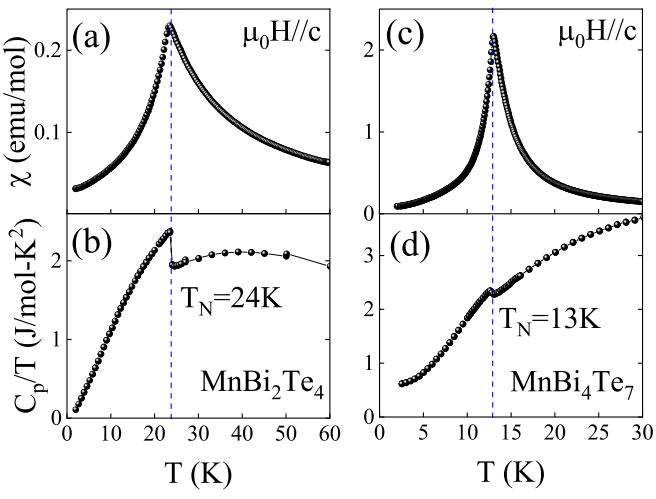

FIG. 2. Temperature dependence of the magnetic susceptibilities of (a) $MnBi_2Te_4$ and (c) $MnBi_4Te_7$ down to 2 K with a magnetic field of 100 Oe under zero-field-cooling condition. Zero-field specific heat of (b) $MnBi_2Te_4$ and (d) $MnBi_4Te_7$ down to 2 K.

Single-crystal neutron diffraction data of $MnBi_4Te_7$ show clearly the appearance of magnetic reflections at the $(H0L + 0.5)$ positions (H, L denote the Miller index) upon cooling below 13 K, confirming the formation of a long-range AFM order. As shown in Fig. 1(c), all magnetic reflections can be indexed by the propagation vector $\mathbf{k} = (0, 0, 1/2)$. Starting with the parent space-group *P*-3*m*1′ and the propagation vector **k** in the A point in the Brillouin zone, through ISODISTORT, two active magnetic irreducible representations mA1- and mA3- were obtained. The magnetic space group P_c-3*c*1 [BNS symbol, basis = (1, 0, 0), (0, 1, 0), (0, 0, 2), origin = (0, 0, 1/2)], generated from the single active mA1-, can be adopted to describe the magnetic structure. The magnetic structure model was refined on the neutron data collected at 4.5 K on DEMAND. The refined magnetic structure is characteristic of an AFM arrangement between the adjacent FM layers, as shown in Fig. 3. The refined total magnetic moment at 4.5 K is $4.01(9)\mu_B$ along the *c* axis, relatively smaller than the value of $5\mu_B$ expected for $S = 5/2$ of Mn^{2+}. Here, the small discrepancy is likely because it is not fully ordered yet at 4.5 K, indicated by the ordering parameter shown below. It appears that $MnBi_4Te_7$ bears a similar spin arrangement between layers (different magnetic symmetry) to $MnBi_2Te_4$ but magnetically orders at a much lower temperature due to the increased distance between magnetic Mn layers.

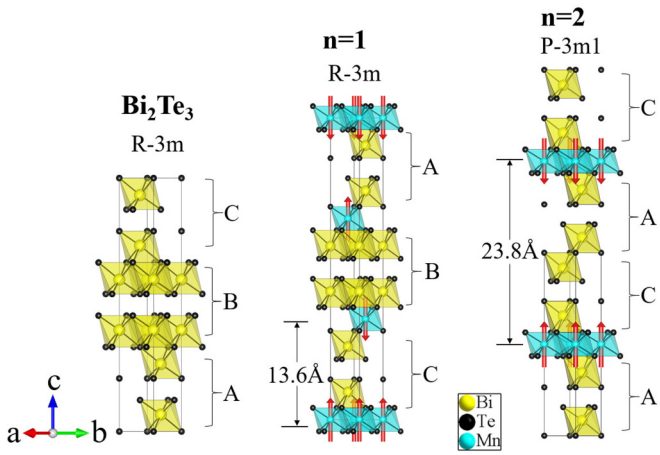

FIG. 3. Schematic drawings of the crystal structures of Bi_2Te_3 and $MnBi_{2n}Te_{3n+1}$ ($n = 1, 2$). Note that for the latter cases, spin arrangements are denoted by red arrows.

The seemingly reduced saturated magnetic moment in both $MnBi_2Te_4$ and $MnBi_4Te_7$ can be reasonably understood by our neutron diffraction results. The deficiency of Mn on the Mn sites in both cases naturally explains the small saturated magnetic moments detected by the bulk magnetization. As determined by the neutron diffraction, the ordered magnetic moment of Mn is reasonably close to the theoretical value.

Having known the magnetic structures of the vdW magnets with $n = 1, 2$, we now examine the temperature dependence of the strongest magnetic reflections for each case. The temperature-dependent intensities of the magnetic reflections$(-1\ 0\ 0.5)$ and $(0\ 1\ 1.5)$ for $MnBi_2Te_4$ and $MnBi_4Te_7$, respectively, are shown in Fig. 4. They follow an empirical power-law behavior [37,38],

$$I = A\left(\frac{T_M - T}{T_M}\right)^{2\beta} + B, \tag{1}$$

where T_M is the critical temperature for the magnetic phase transitions, A is a proportionality constant, β is the order parameter critical exponent, and B is the background. Fits to the power law were performed for two temperature regions for the two cases. The best fit in the temperature ranges of 21–30 K and 9–20 K yields the Neél temperatures $T_N =$ 24.8(1) and 12.5(1) K, and the critical exponents $\beta = 0.50(5)$ and 0.45(3) for $MnBi_2Te_4$ and $MnBi_4Te_7$, respectively. Both critical exponents determined in the two temperature regions that are within the critical regions are in accordance with that of the Ginzburg-Landau theory. In the temperature range of 4.5–21 K, the best fit for $MnBi_2Te_4$ yields the critical exponent $\beta = 0.32(1)$, a value relatively smaller than the results in Ref. [18]. This β value is in fact very close to the value 0.325, expected for a universality class of the three-dimensional Ising model [37]. In the lower-temperature range 4.5 K $< T <$ 9 K, the critical exponent $\beta = 0.32(2)$ of $MnBi_4Te_7$ is very close to that of $MnBi_2Te_4$. This seems to be contradictory to the less three-dimensional magnetism in $MnBi_4Te_7$ caused by the much larger interlayer Mn-Mn distance. The

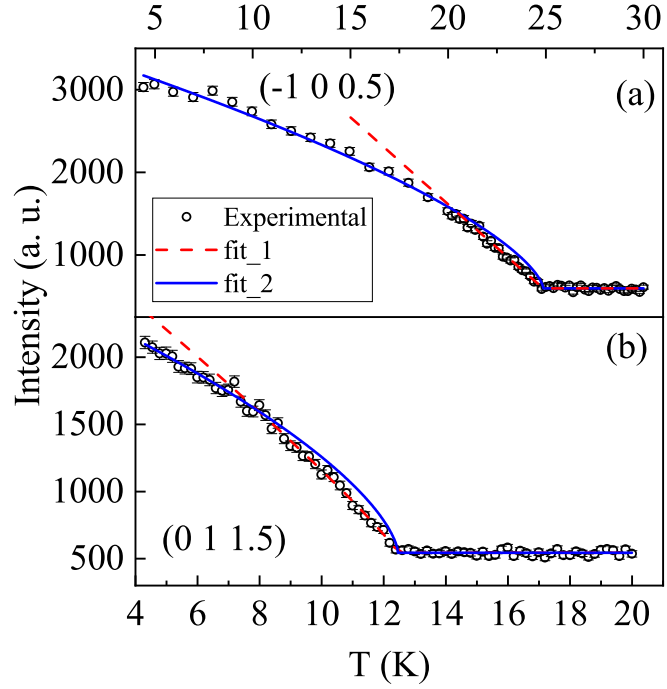

FIG. 4. Magnetic order parameter upon warming at the magnetic reflections $(-1\ 0\ 0.5)$ and $(0\ 1\ 1.5)$ for (a) $MnBi_2Te_4$ and (b) $MnBi_4Te_7$ measured at DEMAND, respectively. Dashed and solid lines represent the results of a power-law fits in different temperature regions.

reason may lie in the fact that the fitting for the $MnBi_4Te_7$ case was done in a temperature range that is relatively close to the critical region which often comes with a crossover from three-dimensional to two-dimensional behavior upon cooling [38,39].

Stacking rule and crystal structures of vdW $MnBi_{2n}Te_{3n+1}$. Based on the crystal structure of $MnBi_2Te_4$ and $MnBi_4Te_7$, as shown in Fig. 3, we can put forward a stacking rule of the crystal structure for this family established on the rhombohedral lattice of Bi_2Te_3. The aforementioned structural description of the Bi_2Te_3 is based on the stacking of three "quintuple-layer" building blocks. This description has been used to predict the infinitely adaptive series of thermoelectric materials [23,40]. However, it seemingly does not capture the essential structural symmetry but rather simply depicts the stacking lattice. As shown in Fig. 3, the crystal structure of Bi_2Te_3 is designated as an A-B-C stacking sequence with A, B, and C representing distinct $[Bi_2Te_3]$ units. Imposed by the inversion and rhombohedral centering translation, the A unit can be progressed into B, and subsequently the C configuration. Simply, we introduce magnetic atoms by substituting M (M denotes the $MnTe_6$ octahedra layer) layers for a $[Bi_2Te_3]$ unit in this A-B-C stacking sequence, giving rise to an infinitely adaptive series $MnBi_{2n}Te_{3n+1}$. Accordingly, we can immediately name the sequence M-C-M-B-M-A-M with $n = 1$ which preserves the crystal symmetry R-3m. This yields the compound $MnBi_2Te_4$, as illustrated in Fig. 3. With $n = 2$, where one more $[Bi_2Te_3]$ unit is added, we get the stacking sequence A-M-C with the space group P-3m1. It corresponds to the compound $MnBi_4Te_7$, indicating a great

compatibility between these structural units. It occurs that the B-type unit occurring in $MnBi_2Te_4$ disappears in $MnBi_4Te_7$. Consequently, this leads to a general stacking rule for a vast number of vdW magnets in this family: The magnetic Mn layer can replace one of the A, B, or C-type units but still leaves the -A-B-C- stacking sequence unchanged. Indeed, with the increment of the value of n ($n \geqslant 1$), the sequence of the building units, crystal symmetry, and lattice parameters of the corresponding vdW magnet can be generated and listed in Table I. Following this stacking rule, one can make an infinitely adaptive series as those listed in Table I (here we only list up to $n = 6$).

Magnetism of $MnBi_{2n}Te_{3n+1}$ derivatives. Recently, theoretical calculations on $MnBi_2Te_4$ [12] have shown that in the (ab) plane the FM interaction between the first nearest neighbors $J_1 = 1.693$ meV strongly dominates over all others. By considering all the exchange interactions in the layer and magnetic anisotropy energy, they suggest the FM ordering temperature of $T_c = 12(1)$ K in a single free-standing $MnBi_2Te_4$ septuple layer [12]. Interestingly, $MnBi_4Te_7$ orders antiferromagnetically at 13 K, very close to the aforementioned 12(1) K. This indicates that in $MnBi_4Te_7$ the intralayer exchange interaction is robust whereas the interlayer one is minimal. Indeed, recent calculations on $MnBi_4Te_7$ yielded that J_1 and $J_\perp$ (a summed exchange coupling between the adjacent layers) [21,22] are 1.704 and -0.150 meV, respectively. With the increase of nonmagnetic building units, FM could be realized by quenching all interlayer exchange interactions. Therefore, for $MnBi_{2n}Te_{3n+1}$ with $n > 2$, if we assume their magnetic ground state to be either A-type AFM or FM with all magnetic moments being aligned along the c axis, the magnetic space group for each compound is predicted and presented in Table I. Experiments to characterize other derivatives and to ascertain the predicted magnetic space groups are called for.

Conclusion. In summary, we have investigated systematically the crystal structure and magnetism of the vdW topological insulators $MnBi_2Te_4$ and $MnBi_4Te_7$. A considerable Mn deficiency has been found on the Mn sites for both cases. Our results have shown that the ordered magnetic moments of $MnBi_2Te_4$ and $MnBi_4Te_7$ are reasonably close to the expected $5\mu_B$ for the Mn^{2+} ion. We have revealed a simple lattice-stacking rule that can lead to an infinitely adaptive series of $MnBi_{2n}Te_{3n+1}$. Although different magnetic symmetry exists in $MnBi_2Te_4$ and $MnBi_4Te_7$ with the former being R_I-3c and the latter being P_c-3c1, our single-crystal neutron diffraction measurements have unambiguously established that in the ordered state, both compounds show the A-type AFM structure with all spins parallel in the ab plane but antiparallel along the c axis, which is critical for the observation of the quantized anomalous Hall effect when they are exfoliated down to a few layers.

Acknowledgments. We thank C. D. Batista for useful discussions. The research at Oak Ridge National Laboratory (ORNL) was supported by the US Department of Energy (DOE), Office of Science, Office of Basic Energy Sciences, Early Career Research Program Award No. KC0402010, under Contract No. DE-AC05-00OR22725 and the U.S. DOE, Office of Science User Facility operated by the ORNL. Work at UCLA was supported by the US Department of Energy (DOE), Office of Science, Office of Basic Energy Sciences under Award No. DE-SC0011978. The U.S. Government retains, and the publisher, by accepting the article for publication, acknowledges that the U.S. Government retains a nonexclusive, paid-up, irrevocable, worldwide license to publish or reproduce the published form of this manuscript, or allow others to do so, for U.S. Government purposes. The Department of Energy will provide public access to these results of federally sponsored research in accordance with the DOE Public Access Plan [41].

[1] A. K. Geim and K. S. Novoselov, The rise of graphene, Nat. Mater. **6**, 183 (2007).

[2] C. Gong, L. Li, Z. Li, H. Ji, A. Stern, Y. Xia, T. Cao, W. Bao, C. Wang, Y. Wang *et al.*, Discovery of intrinsic ferromagnetism in two-dimensional van der Waals crystals, Nature (London) **546**, 265 (2017).

[3] B. Huang, G. Clark, E. Navarro-Moratalla, D. R. Klein, R. Cheng, K. L. Seyler, D. Zhong, E. Schmidgall, M. A. McGurie, D. H. Cobden *et al.*, Layer-dependent ferromagnetism in a van der waals crystal down to the monolayer limit, Nature (London) **546**, 270 (2017).

[4] Y. Tokura, K. Yasuda, and A. Tsukazaki, Magnetic topological insulators, Nat. Rev. Phys. **1**, 126 (2019).

[5] R. S. K. Mong, A. M. Essin, and J. E. Moore, Antiferromagnetic topological insulators, Phys. Rev. B **81**, 245209 (2010).

[6] X.-G. Wen, Choreographed entanglement dances: Topological states of quantum matter, Science **363**, eaal3099 (2019).

[7] J. H. Li, Y. Li, S. Q. Du, Z. Wang, B.-L. Gu, S.-C. Zhang, K. He, W. H. Duan, and Y. Xu, Intrinsic magnetic topological insulators in van der Waals layered $MnBi_2Te_4$-family materials, Sci. Adv. **5**, eaaw5685 (2019).

[8] Y. J. Hao, P. Liu, Y. Feng, X.-M. Ma, E. F. Schwier, M. Arita, S. Kumar, C. Hu, R. Lu, M. Zeng *et al.*, Gapless Surface Dirac Cone in Antiferromagnetomagnetic Topological Insulator $MnBi_2Te_4$, Phys. Rev. X **9**, 041038 (2019).

[9] D. Q. Zhang, M. J. Shi, T. S. Zhu, D. Y. Xing, H. J. Zhang, and J. Wang, Topological Axion States in the Magnetic Insulator $MnBi_2Te_4$ with the Quantized Magnetoelectric Effect, Phys. Rev. Lett. **122**, 206401 (2019).

[10] T. Hirahara, S. V. Eremeev, T. Shirasawa, Y. Okuyama, T. Kubo, R. Nakanishi, R. Akiyama, A. Takayama, T. Hajiri, S.-I. Kimura *et al.*, Large-gap magnetic topological heterostructure formed by subsurface incorporation of a ferromagnetic layer, Nano Lett. **17**, 3493 (2017).

[11] Y. Gong, J. Guo, J. Li, K. Zhu, M. Liao, X. Liu, Q. Zhang, L. Gu, L. Tang, X. Feng *et al.*, Experimental realization of an intrinsic magnetic topological insulator, Chin. Phys. Lett. **36**, 076801 (2019).

[12] M. M. Otrokov, I. P. Rusinov, M. Blanco-Rey, M. Hoffmann, A. Yu. Vyazovskaya, S. V. Eremeev, A. Ernst, P. M. Echenique, A. Arnau, and E. V. Chulkov, Unique Thickness-Dependent Properties of the van der Waals Interlayer

Antiferromagnet $MnBi_2Te_4$ Films, Phys. Rev. Lett. **122**, 107202 (2019).

[13] M. M. Otrokov, I. I. Klimovskikh, H. Bentmann, D. Estyunin, A. Zeugner, Z. S. Aliev, S. Gaß, A. U. B. Wolter, A. V. Koroleva, A. M. Shikin *et al.*, Prediction and observation of an antiferromagnetic topological insulator, Nature **576**, 416 (2019).

[14] A. Zeugner, F. Nietschke, A. U. B. Wolter, S. Gaß, R. C. Vidal, T. R. F. Peixoto, D. Pohl, C. Damm, A. Lubk, R. Hentrich *et al.*, Chemical aspects of the candidate antiferromagnetic topological insulator $MnBi_2Te_4$, Chem. Mater. **31**, 2795 (2019).

[15] B. Chen, F. Fei, D. Zhang, B. Zhang, W. Liu, S. Zhang, P. Wang, B. Wei, Y. Zhang, Z. Zuo *et al.*, Intrinsic magnetic topological insulator phases in the Sb doped $MnBi_2Te_4$ bulks and thin flakes, Nat. Commun. **10**, 4469 (2019).

[16] Y. J. Deng, Y. J. Yu, M. Z. Shi, J. Wang, X. H. Chen, and Y. B. Zhang, Magnetic-field-induced quantized anomalous Hall effect in intrinsic magnetic topological insulator $MnBi_2Te_4$, arXiv:1904.11468.

[17] S. H. Lee, Y. Zhu, Y. Wang, L. Miao, T. Pillsbury, H. Yi, S. Kempinger, J. Hu, C. A. Heikes, P. Quarterman *et al.*, Spin scattering and noncollinear spin structure-induced intrinsic anomalous Hall effect in antiferromagnetic topological insulator $MnBi_2Te_4$, Phys. Rev. Research **1**, 012011 (2019).

[18] J.-Q. Yan, Q. Zhang, T. Heitmann, Zengle Huang, K. Y. Chen, J.-G. Cheng, Weida Wu, D. Vaknin, B. C. Sales, and R. J. McQueeney, Crystal growth and magnetic structure of $MnBi_2Te_4$, Phys. Rev. Mater. **3**, 064202 (2019).

[19] Z. S. Aliev, I. R. Amiraslanov, D. I. Nasonova, A. V. Shevelkov, N. A. Abdullayev, Z. A. Jahangirli, E. N. Orujlu, M. M. Otrokov, N. T. Mamedov, M. B. Babanly, E. V. Chulkov *et al.*, Novel ternary layered manganese bismuth tellurides of the MnTe-Bi_2Te_3 system: Synthesis and crystal structure, J. Alloys Compd. **789**, 443 (2019).

[20] D. Souchay, M. Nentwig, D. Gunther, S. Keilholz, J. de Boor, A. Zeugner, A. Isaeva, M. Ruck, A. U. B. Wolter, B. Buchner, and O. Oeckler, Layered manganese bismuth tellurides with $GeBi_4Te_7$- and $GeBi_6Te_{10}$-type structures: Towards multifunctional materials, J. Mater. Chem. C **7**, 9939 (2019).

[21] C. Hu, K. N. Gordon, P. Liu, J. Liu, X. Zhou, P. Hao, D. Narayan, E. Emmanouilidou, H. Sun, Y. Liu *et al.*, A van der Waals antiferromagnetic topological insulator with weak interlayer magnetic coupling, Nat. Commun. **11**, 97 (2020).

[22] R. C. Vidal, A. Zeugner, J. I. Facio, R. Ray, M. H. Haghighi, A. U. B. Wolter, L. T. C. Bohorquez, F. Caglieris, S. Moser, T. Figgemeier *et al.*, Topological Electronic Structure and Intrinsic Magnetization in $MnBi_4Te_7$: A Bi_2Te_3-Derivative with a Periodic Mn Sublattice, Phys. Rev. X **9**, 041065 (2019).

[23] R. J. Cava, H. Ji, M. K. Fuccillo, Q. D. Gibson, and Y. S. Hor, Crystal structure and chemistry of topological insulators, J. Mater. Chem. C **1**, 3176 (2013).

[24] Y. S. Hor, P. Roushan, H. Beidenkopf, J. Seo, D. Qu, J. G. Checkelsky, L. A. Wray, D. Hsieh, Y. Xia, S.-Y. Xu, D. Qian, M. Z. Hasan, N. P. Ong, A. Yazdani, and R. J. Cava, Development of ferromagnetism in the doped topological insulator $Bi_{2-x}Mn_xTe_3$, Phys. Rev. B **81**, 195203 (2010).

[25] H. J. Zhang, C. X. Liu, X. L. Qi, X. Dai, Z. Fang, and S. C. Zhang, Topological insulators in Bi_2Se_3, Bi_2Te_3 and Sb_2Te_3 with a single Dirac cone on the surface, Nat. Phys. **5**, 438 (2009).

[26] Y. L. Chen, J. G. Analytis, J.-H. Chu, Z. K. Liu, S.-K. Mo, X. L. Qi, H. J. Zhang, D. H. Lu, X. Dai, Z. Fang *et al.*, Experimental realization of a three-dimensional topological insulator, Bi_2Te_3, Science **325**, 178 (2009).

[27] V. V. Atuchin, T. A. Gavrilova, K. A. Kokh, N. V. Kuratieva, N. V. Pervukhina, and N. V. Surovtsev, Structural and vibrational properties of PVT grown Bi_2Te_3 microcrystals, Solid State Commun. **152**, 1119 (2012).

[28] F. Ye, Y. Liu, R. Whitfield, R. Osborn, and S. Rosenkranz, Implementation of cross correlation for energy discrimination on the time-of-flight spectrometer CORELLI, J. Appl. Crystallogr. **51**, 315 (2018).

[29] See Supplemental Material at http://link.aps.org/supplemental/10.1103/PhysRevB.101.020412 for experimental methods and the description of the crystal structure refinement and magnetic structure determination.

[30] B. C. Chakoumakos, H. B. Cao, F. Ye, A. D. Stoica, M. Popovici, M. Sundaram, W. Zhou, J. S. Hicks, G. W. Lynn, and R. A. Riedel, Symmetry-based computational tools for magnetic crystallography, J. Appl. Crystallogr. **44**, 655 (2011).

[31] H. B. Cao, B. C. Chakoumakos, K. M. Andrews, Y. Wu, R. A. Riedel, J. Hodges, W. D. Zhou, R. Gregory, B. Haberi, J. Molaison, and G. W. Lynn, DEMAND, a dimensional extreme magnetic neutron diffractometer at the High Flux Isotope Reactor, Crystals **9**, 5 (2019).

[32] J. Rodríguez-Carvajal, Recent advances in magnetic structure determination by neutron powder diffraction, Physica B: Condens. Matter **192**, 55 (1993).

[33] D. S. Lee, T.-H. Kim, C.-H. Park, C.-Y. Chung, Y. S. Lim, W.-S. Seo, and H.-H. Park, Crystal structure, properties and nanostructuring of a new layered chalcogenide semiconductor, Bi_2MnTe_4, CrystEngComm **15**, 5532 (2013).

[34] N. V. Belov, N. N. Neronova, and T. S. Smirnova, Shubnikov groups, Sov. Phys. Crystallogr. **2**, 311 (1957).

[35] B. J. Campbell, H. T. Stokes, D. E. Tanner, and D. M. Hatch, ISODISPLACE: An internet tool for exploring structural distortions, J. Appl. Crystallogr. **39**, 607 (2006).

[36] J. M. Perez-Mato, S. V. Gallego, E. S. Tasci, L. Elcoro, G. de la Flor, and M. I. Aroyo, Symmetry-based computational tools for magnetic crystallography, Annu. Rev. Mater. Res. **45**, 217 (2015).

[37] S. G. Brush, History of the Lenz-Ising model, Rev. Mod. Phys. **39**, 883 (1967).

[38] R. J. Birgeneau, H. J. Guggenheim, and G. Shirane, Neutron scattering investigation of phase transitions and magnetic correlations in the two-dimensional antiferromagnets K_2NiF_4, Rb_2MnF_4, Rb_2FeF_4, Phys. Rev. B **1**, 2211 (1970).

[39] A. R. Wildes, H. M. Rønnow, B. Roessli, M. J. Harris, and K. W. Godfrey, Static and dynamic critical properties of the quasi-two-dimensional antiferromagnet $MnPS_3$, Phys. Rev. B **74**, 094422 (2006).

[40] J. W. G. Bos, H. W. Zandbergen, M.-H. Lee, N. P. Ong, and R. J. Cava, Structures and thermoelectric properties of the infinitely adaptive series $(Bi_2)_m(Bi_2Te_3)_n$, Phys. Rev. B **75**, 195203 (2007).

[41] https://www.energy.gov/downloads/doe-public-access-plan.

Correction: Several entries in Table I contained errors in or omissions of magnetic space group notation and have been fixed.